NEURAL REGENERATION RESEARCH
February 2015, Volume 10, Issue 2
www.nrronline.org

RESEARCH ARTICLE

MicroRNA-9 promotes the neuronal differentiation of rat bone marrow mesenchymal stem cells by activating autophagy

Guang-yu Zhang[1], Jun Wang[1], Yan-jie Jia[2], Rui Han[3], Ping Li[1], Deng-na Zhu[1, *]

1 Rehabilitation and Treatment Center for Children with Cerebral Palsy of Henan Province, the Third Affiliated Hospital of Zhengzhou University, Zhengzhou, Henan Province, China
2 Department of Neurology, the First Affiliated Hospital of Zhengzhou University, Zhengzhou, Henan Province, China
3 Department of Pediatrics, the Third Affiliated Hospital of Zhengzhou University, Zhengzhou, Henan Province, China

***Correspondence to:**
Deng-na Zhu, M.D., zhudengna@126.com.

***doi:**10.4103/1673-5374.143439*
***http:**//www.nrronline.org/*

***Accepted:** 2014-08-25*

Abstract

MicroRNA-9 (miR-9) has been shown to promote the differentiation of bone marrow mesenchymal stem cells into neuronal cells, but the precise mechanism is unclear. Our previous study confirmed that increased autophagic activity improved the efficiency of neuronal differentiation in bone marrow mesenchymal stem cells. Accumulating evidence reveals that miRNAs adjust the autophagic pathways. This study used miR-9-1 lentiviral vector and miR-9-1 inhibitor to modulate the expression level of miR-9. Autophagic activity and neuronal differentiation were measured by the number of light chain-3 (LC3)-positive dots, the ratio of LC3-II/LC3, and the expression levels of the neuronal markers enolase and microtubule-associated protein 2. Results showed that LC3-positive dots, the ratio of LC3-II/LC3, and expression of neuron specific enolase and microtubule-associated protein 2 increased in the miR-9^{+} group. The above results suggest that autophagic activity increased and bone marrow mesenchymal stem cells were prone to differentiate into neuronal cells when miR-9 was overexpressed, demonstrating that miR-9 can promote neuronal differentiation by increasing autophagic activity.

***Key Words:** nerve regeneration, microRNA-9; bone marrow mesenchymal stem cells; differentiation; neuron-like cells; autophagy; neuron specific enolase; microtubule-associated protein; LC3; neural regeneration*

***Funding:** This study was supported by a grant from the Science and Technology Bureau of Zhengzhou City in China, No. 121PPTGG507-11 and the National Natural Science Foundation of China, No. 81071114, 81371385.*

Zhang GY, Wang J, Jia YJ, Han R, Li P, Zhu DN (2015) MicroRNA-9 promotes the neuronal differentiation of rat bone marrow mesenchymal stem cells by activating autophagy. Neural Regen Res 10(2):314-320.

Introduction

Bone marrow mesenchymal stem cells are multipotent stem cells, and can differentiate into many cell types, such as osteocytes, chondrocytes, adiocytes, and neural cells (Bianco et al., 2008). Neuronal cell differentiation from bone marrow mesenchymal stem cells may be a promising treatment choice for nervous system disorders, including neurodegenerative diseases and hypoxic ischemic encephalopathy. The precise mechanism underlying neuronal differentiation, however, remains poorly understood (Cho et al., 2005; Lee et al., 2010). MicroRNAs are small endogenous single-stranded RNA, and at the transcriptional level can regulate gene expression (Elramah et al., 2014). In mouse cortical neurons, microRNA-9 (miR-9) controls axon development through modulating Map1b expression (Dajas-Bailador et al., 2012). MiR-9 exerts a critical effect on the differentiation of neural progenitor cells through suppressing the expression of monocyte chemotactic protein-induced protein 1 and subsequent downstream activation of nuclear factor-kappa B and cyclic adenosine monophosphate response element-binding protein pathways (Yang et al., 2013). Studies have confirmed that miR-9 expression is very abundant in brain tissue, and promotes neural stem cell differentiation through suppressing *Hes-1* gene expression (Tan et al., 2012). Our previous study found that miR-9 contributed to the neuronal differentiation of bone marrow mesenchymal stem cells, but the underlying mechanism is not clear (Han et al., 2012).

Autophagy is the self-degradation process of cellular contents, in which proteins and organelles are enclosed in autophagosomes and degraded upon fusing with lysosomal components, by which cells produce small molecular substances for the synthesis of macromolecules or adenosine 5′-triphosphate generation (Ryter et al., 2014). Autophagy can be induced by starvation and other stresses to act as a recycling system which is essential for cellular homeostasis and renovation (Ahn et al., 2014). Meanwhile, accumulating evidence has shown that autophagy has critical roles in stem cell differentiation (Vessoni et al., 2012). Autophagy is reported to interact with crucial developmental pathways, such as Wnt, transforming growth factor-β and fibroblast growth

factor. This suggests that autophagy possibly regulates cell fate decisions, such as differentiation and proliferation (Zhang et al., 2012; Petherick et al., 2013; Ding et al., 2014). When autophagic activity increased, efficiency of neuronal differentiation improved (Zhang et al., 2013). MicroRNAs regulate autophagic activity *via* modulating autophagy-related genes (Atgs) and their regulators (Zhu et al., 2009; Jian et al., 2011; Wan et al., 2014), but it remains unclear whether miR-9 regulates autophagic activity during bone marrow mesenchymal stem cell differentiation. Therefore, this study sought to explore the changes in autophagic activity and neuronal differentiation efficiency at different expression levels of miR-9, and to investigate the mechanism of miR-9 in the promotion of bone marrow mesenchymal stem cell differentiation into neurons.

Materials and Methods

Animals

A total of 10 Wistar rats, of either gender, aged 6–8 weeks and weighing 150–200 g, were purchased from the Experimental Animal Center of Henan Province, China (License No. SCXK (Yu) 2005-0001). Experimental procedures were approved by the Animal Ethics Committee of Zhengzhou University, China.

Cell culture

The femur and tibia from both hindlimbs were dissected from rats, and the marrow cavity was exposed by cutting the end of each bone. Dulbecco's modified Eagle's medium (DMEM; Invitrogen, Carlsbad, CA, USA) was used to flush the bones. Cells were maintained in a complete medium consisting of DMEM and 10% fetal bovine serum (Invitrogen). Twenty-four hours later, the complete culture medium was replaced and the adherent cells were seen on the wall of the flask. From then on, the complete culture medium was replaced every 3–4 days. When cells were 70–80% confluent, 0.25% trypsin containing 0.04% ethylenediamine tetraacetic acid (Invitrogen) was used to detach the cells from the wall of the flask. The cells were suspended and reseeded continuously. Bone marrow mesenchymal stem cells were gradually purified with subculture, and passage 4 bone marrow mesenchymal stem cells have been shown to produce pure cultures (Jia et al., 2009). We therefore selected passage 5 bone marrow mesenchymal stem cells for our study.

Experimental groups

Bone marrow mesenchymal stem cells were divided into four groups: miR-9$^+$ group (transfected with MiR-9-1-LV), untransfected group, miR-9$^-$ group (transfected with anti-mmu-miR-9-1 inhibitor), and the negative control group (transfection reagent was added without miRNA inhibitor). Cells were cultured in 24-well plates. Each group contained six wells, and 5×10^4 cells were added into each well. The experiment was repeated in triplicate.

MiR-9-1 lentiviral vector transfection

Before transfection, bone marrow mesenchymal stem cells were digested and suspended, and 5×10^4 cells were added into each well of the 24-well plates. Forty-eight hours later, miR-9-1 lentiviral vector (Genechem, Shanghai, China) was added into the wells, and the multiplicity of infection was 30. Bone marrow mesenchymal stem cells were then cultured for 24–96 hours (Han et al., 2012). The fluorescence expression was monitored with an inverted fluorescent microscope (Leica, Solms, Germany) to assess transfection efficiency.

Anti-mmu-miR-9-1 inhibitor transfection

In accordance with the instructions for the Anti-mmu-miR-9-1 inhibitor labeled with AlexaFluor 488 (Qiagen, Frankfurt, Germany), when bone marrow mesenchymal stem cell confluence reached 50–70%, 1.5 μL miRNA inhibitor was diluted in 100 μL culture medium without serum. HiPerFect transfection reagent (3 μL; Qiagen) was added to the diluted miRNA inhibitor and mixed by vortexing. The complexes were incubated for 8 minutes at room temperature, and were then added onto the cells to a final miRNA inhibitor concentration of 50 nM. Cells were incubated with transfection complexes for 48–72 hours under normal growth conditions (Han et al., 2012).

Neuronal differentiation of bone marrow mesenchymal stem cells *in vitro*

At 72 hours after transfection, according to Woodbury's method (Woodbury et al., 2000), when bone marrow mesenchymal stem cells grew to 50–70% confluence, the complete culture medium was replaced by pre-induction medium, supplemented with 1 mM β-mercaptoethanol (Amresco, Solon, OH, USA), 10% fetal bovine serum (Invitrogen) and DMEM (Invitrogen). Twenty-four hours later, the pre-induction medium was replaced by induction medium consisting of DMEM (Invitrogen) and 10 mM β-mercaptoethanol (Invitrogen). Cells were maintained in the induction medium for 6 days. The morphological alterations in bone marrow mesenchymal stem cells were observed using an inverted microscope (Leica) during the induction process.

3-(4,5-Dimethylthiazol-2-yl)-2,5-diphenyltetrazolium bromide (MTT) assay

Cell viability was assessed by MTT (Beyotime, Shanghai, China) assay. MTT assay was performed at 0, 24, 48, and 72 hours after transfection. Bone marrow mesenchymal stem cells were seeded in 96-well plates at a density of 1×10^4 cells/well (100 μL/well). Then 20 μL MTT (5 mg/mL) was added in each well, and maintained for 4 hours. The medium was removed, and 200 μL dimethyl sulfoxide (Dingguo, Beijing, China) was added in each well, followed by 10 minutes of oscillation. Optical density at 490 nm was measured using an enzyme linked immunosorbent assay. Cell survival rates were calculated by the ratio of absorbance between the transfection group and the untransfected group.

Real-time PCR for detection of miR-9 expression

Total RNA was extracted from cells using the miRcute miRNA isolation Kit (Tiangen, Beijing, China) at 72 hours after

Table 1 Primer sequence

Gene	Sequence	Product size (bp)
miR-9-1	Forward: 5′-TCA TAA AGC TAG ATA ACC GAA GAT-3′ Reverse: 5′-TCC AGA GGC GAC CCA GAG C-3′	405
5s	Forward: 5′-TCT CGT CTG ATC TCG GAA GC-3′ Reverse: 5′-AGC CTA CAG CAC CCG GTA TT-3′	120

transfection. MiR-9-1 and internal reference 5s sequences (Ribobio, Guangzhou, China) are shown in **Table 1**. MiRNA Reverse Transcription system (Promega, Beijing, China) was used for the reverse transcription of miRNA to cDNA. Gotaq qPCR Master Mix (Promega) was used to subject cDNA to quantitative real-time PCR. Relative miR-9 expression ($2^{-\Delta\Delta Ct}$) was quantified according to the previous method (Li et al., 2013), and compared among different groups.

Immunofluorescence staining

At 6 days after induction, cells were washed three times with PBS (Dingguo), fixed in 100% methanol for 10 minutes at −20°C and then blocked by immunostaining blocking buffer (Beyotime) for 1 hour. Cells were then incubated with primary antibodies including rabbit anti-neuron specific enolase (1:100; Santa Cruz Biotechnology, Santa Cruz, CA, USA), rabbit anti-microtubule-associated protein 2 (1:100; Santa Cruz Biotechnology), and rabbit anti-microtubule-associated protein 1 light chain-3B (LC3B; 1:100; Cell Signaling, Boston, MA, USA) polyclonal antibodies overnight at 4°C. Subsequently, cells were washed three times with PBS, incubated in Cy3-labeled goat anti-rabbit IgG (Santa Cruz Biotechnology) at room temperature for 2 hours, and then visualized with a fluorescent microscope (Leica) and a confocal microscope (Zeiss, Oberkochen, Germany). Twelve fields of each well were randomly selected at a magnification of 400× under the light microscope (Leica), and the total number of the cells was counted. The numbers of positive cells were counted under a fluorescent microscope (Leica) in the same field, and the percentage of positive cells was calculated using the ratio of positive cells in the total cells.

Western blot assay

At 6 days after induction, cells were washed three times with PBS, and treated with cell lysis buffer (Beyotime). Cell lysate (20 μL) was loaded onto sodium dodecyl sulfate polyacrylamide gel, and electro-transferred to polyvinylidene fluoride membrane (Merck Millipore, Darmstadt, Germany). The membrane was blocked by blocking buffer (Cwbio, Beijing, China) at room temperature for 2 hours, and incubated with the primary antibodies: rabbit anti-LC3B (1:1,000; Cell Signaling), rabbit anti-neuron specific enolase (1:1,000; Santa Cruz Biotechnology), rabbit anti-microtubule-associated protein 2 (1:1,000; Santa Cruz Biotechnology), and rabbit anti-β-actin (1:1,000; Santa Cruz Biotechnology) polyclonal antibodies overnight at 4°C. The membrane was then incubated with bovine anti-rabbit IgG, horseradish peroxidase-linked antibody (1:2,000; Santa Cruz Biotechnology) for 2 hours at room temperature, with enhanced chemiluminescence reagents (Santa Cruz Biotechnology) for 1 minute, followed by exposing the membrane to X-ray film (Dingguo). Gray scale densitometric scanning of the protein bands was performed with ImageJ 1.42q software (National Institutes of Health, Washington, DC, USA). The relative expression of target proteins was expressed as a ratio of grey values, which was the gray value ratio of target proteins and β-actin (Santa Cruz Biotechnology).

Statistical analysis

All data were analyzed by using SPSS 17.0 software (SPSS, Chicago, IL, USA) and reported as the mean ± SD. One-way analysis of variance was used for the multiple comparisons, and least significant difference test was applied for paired comparison. A value of $P < 0.05$ was considered statistically significant.

Results

MiR-9 promoted the differentiation of bone marrow mesenchymal stem cells into neurons

Gain- and loss-of-function strategies were adopted to determine the effects of miR-9 on neuronal differentiation of bone marrow mesenchymal stem cells. Bone marrow mesenchymal stem cells were transfected with miR-9 lentiviral vector to investigate if miR-9 gain-of-function promotes neuronal differentiation of bone marrow mesenchymal stem cells. This study also transfected anti-mmu-miR-9-1 inhibitors into bone marrow mesenchymal stem cells to construct loss-of-function. At 24 hours after transfection, green fluorescence was seen in miR-9$^+$ group and miR-9$^-$ group under a fluorescent microscope. The strongest fluorescence was seen at 72 hours after transfection in both the miR-9$^+$ and miR-9$^-$ groups (**Figure 1A**). Real-time PCR results showed that the relative expression of miR-9 was higher in the miR-9$^+$group than in the other groups ($P < 0.05$; **Figure 1B**). There were similar expression levels in miR-9 between the untransfected group and the negative control group. MTT assay results showed that cell survival rates decreased at 24 hours after transfection, and survival rates improved at 48 and 72 hours (**Figure 1C**).

Bone marrow mesenchymal stem cells were induced by β-mercaptoethanol for 6 days. The morphology of bone marrow mesenchymal stem cells constricted and emitted cellular processes at 24 hours. The majority of cells became typically neuron-like at 6 days after induction (**Figure 2A**).

To investigate neurogenesis, immunofluorescence and western blot assay were applied to analyze the expression of neuron specific enolase and microtubule-associated protein 2 after induction. The percentage of neuron specific enolase- and microtubule-associated protein 2-positive cells in the miR-9$^+$ group was greater than the other groups ($P < 0.05$; **Figure 2A**, **C**), and there was a similar percentage of neuron specific enolase- and microtubule-associated protein 2-posi-

tive cells between the untransfected group and the negative control group (**Figure 2A**, **C**). Western blot assay results revealed that the expression of neuron specific enolase and microtubule-associated protein 2 in the miR-9$^+$ group was highest compared with the other groups ($P < 0.05$; **Figure 2B**, **D**). The expression levels of neuron specific enolase and microtubule-associated protein 2 in the untransfected group were similar to the negative control group (**Figure 2B**, **D**). These data confirmed that miR-9 could promote the differentiation of bone marrow mesenchymal stem cells into neurons.

Autophagy is regulated by miR-9 in neuronal differentiation of bone marrow mesenchymal stem cells

LC3 is a widely accepted marker of autophagy. During the induction of autophagy, the cytosolic form of LC3 (LC3-I) is conjugated with phosphatidylethanolamine and becomes LC3-II (Zeng and Zhou, 2008). The degree of autophagosome formation can be measured using the LC3-II/LC3-I ratio or the expression level of LC3-II, and LC3-positive dots are also a good marker of autophagosome formation (Mizushima and Yoshimori, 2007). Immunofluorescence staining exhibited more LC3-positive dots in the miR-9$^+$ group than the other groups ($P < 0.05$; **Figure 3A**, **C**). The untransfected and negative control groups had similar numbers of LC3-positive dots (**Figure 3A**, **C**). The results of the western blot assay showed that expression of LC3-II and the LC3-II/LC3-I ratio was higher in miR-9$^+$ group than in the other groups, and the lowest expression level of LC3-II and LC3-II/LC3-I ratio were shown in the miR-9$^-$ group ($P < 0.05$; **Figure 3B**, **D**). There were similar ratios of LC3-II/LC3-I between the untransfected and negative control groups (**Figure 3B**, **D**). The above results suggested that autophagy might be regulated by miR-9 during the neuronal differentiation of bone marrow mesenchymal stem cells.

Discussion

MicroRNAs have critical roles in stem cell maintenance, renewal and self-differentiation (Zhao et al., 2009). Nuclear receptor TLX is an essential regulator for neuronal stem cell self-renewal, and miR-9 promotes neuronal stem cell differentiation by suppressing TLX expression (Zhao et al., 2009). In the developing zebrafish brain, miR-9 directly suppresses antagonistic factor to control the time of neurogenesis (Coolen et al., 2012). Krichevsky et al. (2006) have found that miR-9 expression was highest in the fifth stage of embryonic development, which is the critical period of neuronal precursors differentiating into neurons and glial cells. The number of neurons generated from neuronal precursors was reduced by 29–31% when miR-9 was suppressed by chemical substances (Krichevsky et al., 2006). Recent studies also verified that miR-9 possibly plays an important role in bone marrow mesenchymal stem cell differentiation into neurons (Jing et al., 2011; Han et al., 2012). To investigate miR-9 effects on the neuronal differentiation of bone marrow mesenchymal stem cells, miR-9-1 lentiviral vector and miR-9-1 inhibitor were utilized to regulate miR-9 expression. The expression of neuronal markers neuron specific enolase and microtubule-associated protein 2 increased when miR-9 was overexpressed, indicating that miR-9 contributed to the neuronal differentiation of bone marrow mesenchymal stem cells, however, the exact mechanism was complex.

Autophagy is a non-selective degradation pathway, by which proteins and organelles are degraded, which is important for the maintenance of intracellular homeostasis (Mizushima et al., 2008). Meanwhile, there is increasing evidence indicating autophagy also plays crucial roles in differentiation. Zhao et al. (2010) found autophagy activity markedly increased after glioma stem/progenitor cells were induced by fetal calf serum to differentiate, and autophagy activator effectively promoted the differentiation of glioma stem/progenitor cells. Autophagy exerts a key effect on hypoxia-induced osteoclastogenesis *in vitro*. Autophagic activity increased when RAW264.7 cells differentiated into osteoclasts. The osteoclast differentiation of RAW264.7 cells was inhibited when autophagy was suppressed by 3-methyladenine (Zhao et al., 2012). Rapamycin is an activator of autophagy, can enhance neuronal differentiation of NG108-15 neuroblastoma cells, which suggested that autophagy promoted neuronal differentiation (Chin et al., 2010). *Atg7*, *Becn1*, *Ambra1* and *LC3* are important autophagy genes (Yu et al., 2004). A previous study demonstrated that the expression of the above autophagy genes increase during the initial period of neuronal differentiation at embryonic 15.5 in the mouse embryonic olfactory bulb. Additionally, autophagic flux was observed during the neuronal differentiation of olfactory bulb-derived stem/progenitor cells. 3-Methyladenine or wortmannin, inhibitors of autophagy, disrupt neurogenesis of olfactory bulb-derived stem/progenitor cells (Vázquez et al., 2012). New morphology and functions were generally seen in differentiated cells, involving significant morphological and structural changes, therefore requiring large amounts of adenosine 5′-triphosphate, breakdown and recycling of cellular components (Levine et al., 2004; Vessoni et al., 2012). Autophagy recycles cellular components for biosynthesis or adenosine 5′-triphosphate generation to meet demands, thus supporting differentiation (Michaeli and Galili, 2014). Accumulating evidence has recently revealed that miRNAs modulate autophagic activity at different autophagic stages. To examine whether miR-9 regulates autophagic activity during the neuronal differentiation of bone marrow mesenchymal stem cells, immunofluorescence was applied to measure the number of LC3-positive dots and western blot assay was applied to measure the ratio of LC3-II/LC3-I. The results showed that the number of LC3-positive dots and the ratio of LC3-II/LC3-I was significantly higher in the miR-9$^+$ group compared with the other groups after induction, which indicated that autophagy activity increased when miR-9 was overexpressed, and suggested that autophagy was regulated by miR-9. Our previous study confirmed that neuronal differentiation efficiency increased greatly when bone marrow mesenchymal stem cells were induced by β-mercaptoethanol and autophagy inducer, while

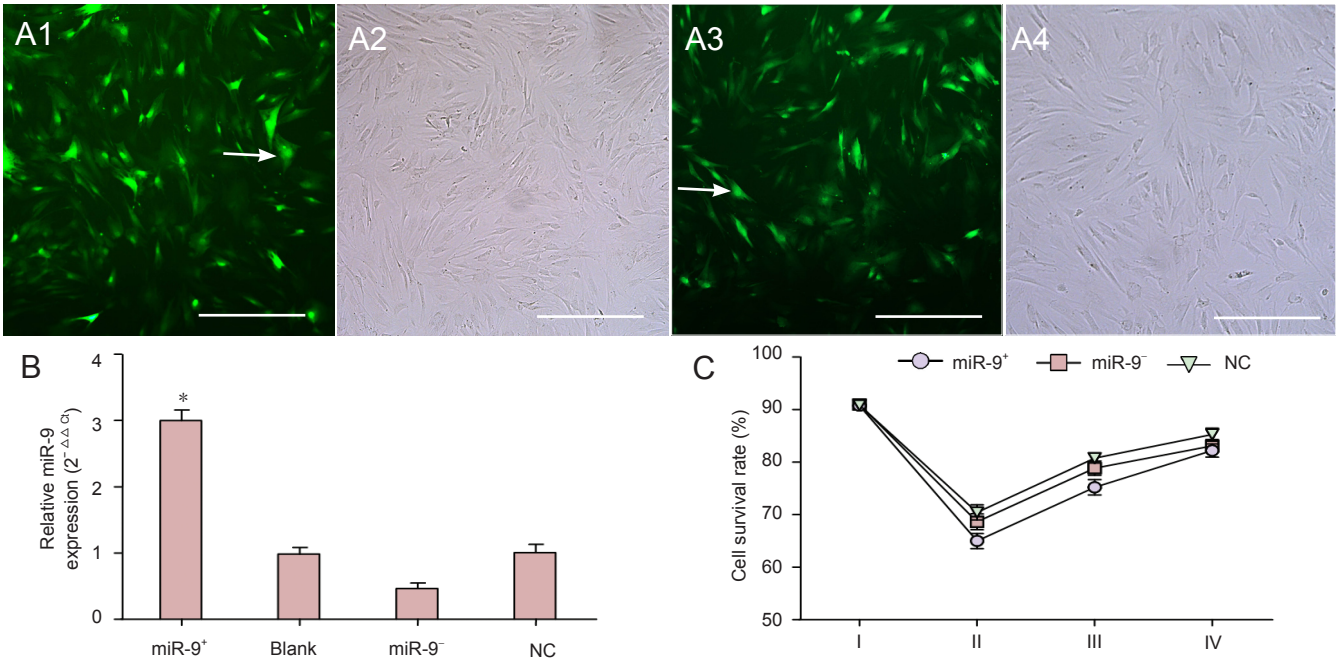

Figure 1 MiR-9-1 lentiviral vector and miR-9-1 inhibitor transfection.
(A1–4) Green fluorescence was strongest at 72 hours after transfection with miR-9-1 lentiviral vector or miR-9-1 inhibitor (inverted fluorescent microscope; scale bars: 250 μm). Green signal in the miR-9$^+$ group indicates green fluorescent protein (GFP) and the green staining in the miR-9$^+$ group indicates AlexaFluor 488 staining. Arrows show GFP-positive and AlexaFluor 488-positive BMSCs. (B) Real time-PCR showed that the relative expression ($2^{-\Delta\Delta Ct}$) of miR-9 in the miR-9$^+$ group was greater than in the other groups (*$P < 0.05$). (C) MTT assay showed that the cell survival rates decreased at 24 hours after transfection in BMSCs compared with untransfected BMSCs ($P < 0.05$). Survival rates improved at 48 and 72 hours, but still remained lower than untransfected BMSCs ($P < 0.05$). Data are expressed as the mean ± SD. Intergroup comparison was performed using one-way analysis of variance followed by the least significant difference test. I: Before transfection; II: 24 hours after transfection; III: 48 hours after transfection; IV: 72 hours after transfection; Blank: untransfected group; NC: negative control group; miR-9: microRNA-9; MTT: 3-(4,5-dimethylthizol-2-yl)-2,5-diphenyltetrazolium bromide; BMSCs: bone marrow mesenchymal stem cells.

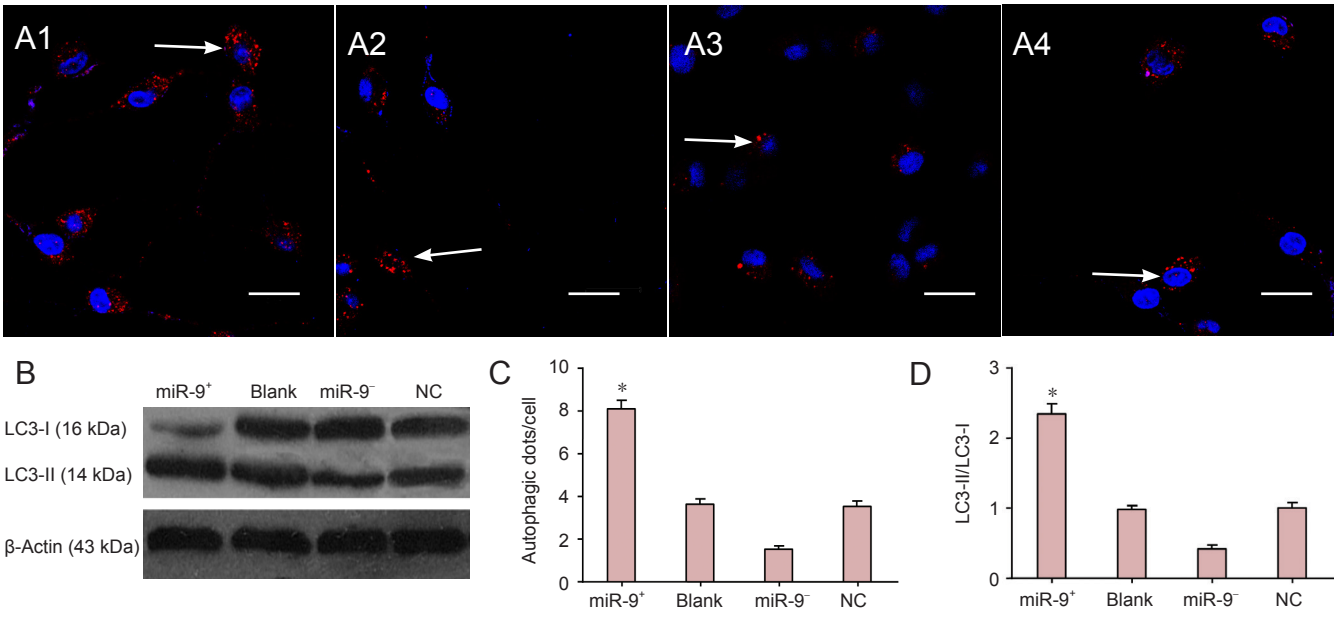

Figure 3 Expression of autophagic marker LC3 in differentiated BMSCs.
(A1–4, C) Immunofluorescence staining of LC3 in differentiated BMSCs (confocal microscope; scale bar: 20 μm). Red indicates Cy3 staining and blue indicates 4′,6-diamidino-2-phenylindole (DAPI) staining. Arrows show LC3-positive dots. The number of LC3-positive dots in the miR-9$^+$ group was greater than in other groups at 400× magnification (*$P < 0.05$). There were similar numbers of LC3-positive dots between the blank group and the NC group. (B) Western blot assay for the detection of the expression of LC3-I and LC3-II in differentiated BMSCs. (D) Quantification of LC3-II/LC3-I ratio. *$P < 0.05$, *vs.* other groups. Data are expressed as the mean ± SD. Intergroup comparison was performed using one-way analysis of variance followed by the least significant difference test. BMSCs: Bone marrow mesenchymal stem cells; miR-9: microRNA-9; blank: untransfected group; NC: negative control group; LC3: light chain-3.

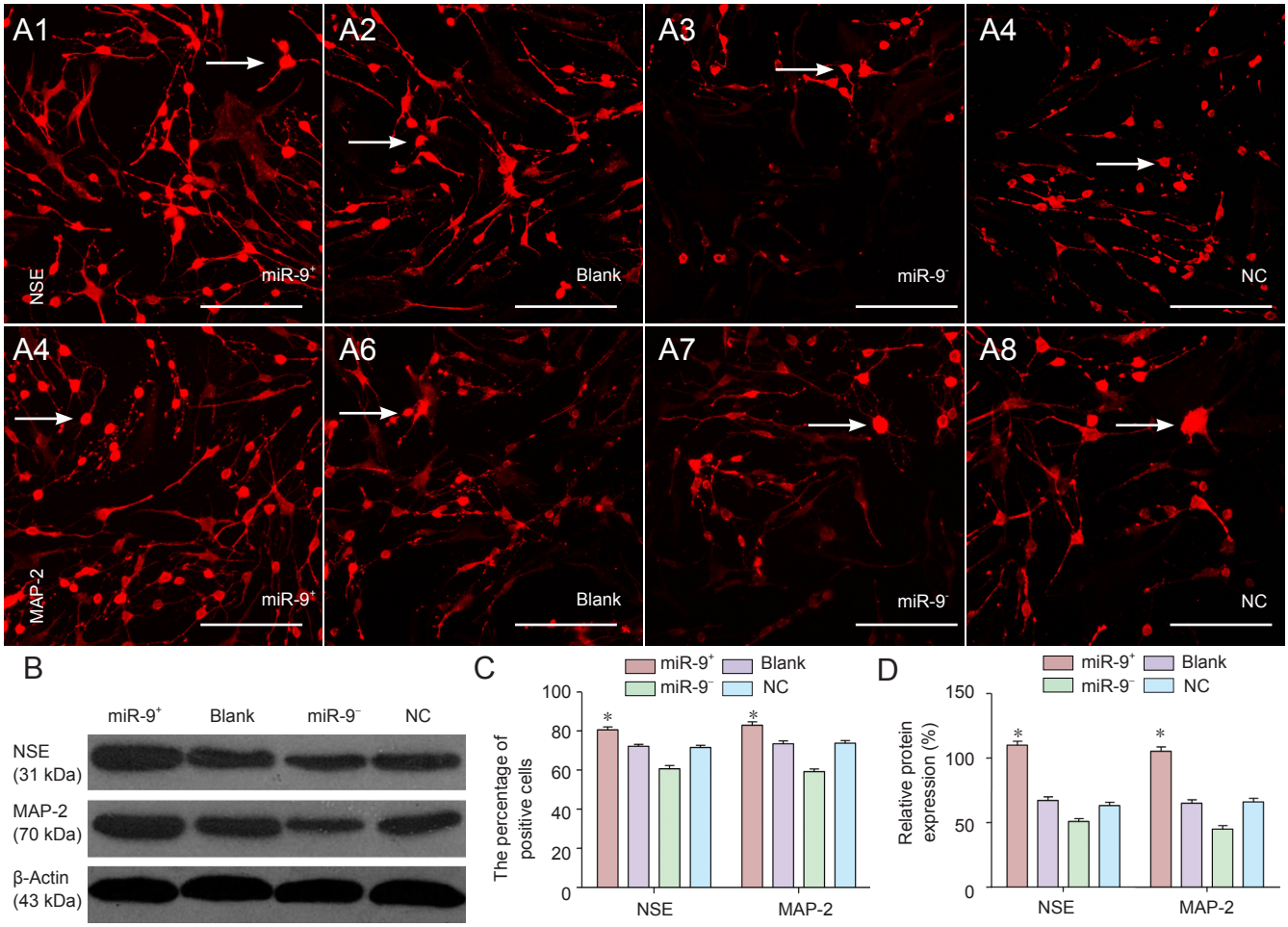

Figure 2 Expression of neuronal markers MAP-2 and NSE in differentiated BMSCs.
(A1–8) Immunofluorescence staining of MAP-2 and NSE in differentiated BMSCs (inverted fluorescent microscope; scale bars: 250 μm). Red indicates Cy3 staining. Arrows show MAP-2- and NSE-positive neuronal cells. (B) Western blot assay for detecting the expression of NSE and MAP-2 in differentiated BMSCs. (C) The percentages of NSE- and MAP-2-positive cells in the miR-9$^+$ group were significantly higher than in other groups at 400× magnification (*$P < 0.05$). No difference was detected between the blank group and the NC group. (D) Protein expression of neuronal markers. *$P < 0.05$, *vs.* other groups. Data are expressed as gray value ratio of target protein to β-actin (mean ± SD). Intergroup comparison was performed using one-way analysis of variance followed by the least significant difference test. NSE: Neuron specific enolase; MAP-2: microtubule-associated protein 2; miR-9: microRNA-9; BMSCs: bone marrow mesenchymal stem cells; Blank: untransfected group; NC: negative control group.

neuronal differentiation efficiency decreased when bone marrow mesenchymal stem cells were induced by β-mercaptoethanol and autophagy inhibitor, which suggested that the increased autophagic activity promotes the differentiation of bone marrow mesenchymal stem cells into neurons (Zhang et al., 2013). Taken together, the above-described results indicated that miR-9 might promote neuronal differentiation by increasing autophagic activity.

Though the study confirmed that miR-9 promoted neuronal differentiation by modulating autophagic activity, this study did not explore the downstream mechanism of this observation. Recent studies show that miRNAs modulate some Atgs and their regulators to regulate autophagic activity. MiR-216b inhibits the expression of Beclin-1 activity to suppress autophagy (Xu et al., 2014). LC3/Atg8 is one of ubiquitin-like proteins which are essential for the formation of autophagosomes. In this process, miR-183 and miR-204 suppress the activation of LC3-I and LC3-II to disrupt autophagosome formation (Abraham et al., 2011; Jian et al., 2011). In the pathogenesis of Crohn's disease, miR-106B and miR-93 are found to inhibit ATG16L1 expression and to reduce autophagic activity, which prevents removal of bacteria from epithelial cells (Lu et al., 2014). Mammalian target of rapamycin functions as a negative regulator of autophagy. Rheb directly interacts with mammalian target of rapamycin to increase its activity. By contrast, miR-155 inhibits Rheb expression to accelerate autophagic activity (Wang et al., 2013). Thus, the precise mechanisms underlying miR-9 modulating autophagic activity are complex, and need further study.

In conclusion, miR-9 can promote neuronal differentiation by modulating autophagic activity, and may help us to further investigate the mechanisms underlying cell differentiation and to promote bone marrow mesenchymal stem cell-based therapy for treatment of nervous system diseases.

Author contributions: *GYZ completed the experiments and wrote the manuscript. DNZ provided research ideas and research design. JW, YJJ, RH and PL guided the study and they were responsible for data analysis and participated in the study. All authors approved the final version of the paper.*
Conflicts of interest: *None declared.*

References

Abraham D, Jackson N, Gundara JS, Zhao J, Gill AJ, Delbridge L, Robinson BG, Sidhu SB (2011) MicroRNA profiling of sporadic and hereditary medullary thyroid cancer identifies predictors of nodal metastasis, prognosis, and potential therapeutic targets. Clin Cancer Res 17:4772-4781.

Ahn S, Park J, An I, Jung SJ, Hwang J (2014) Transient Receptor Potential Cation Channel V1 (TRPV1) is degraded by starvation- and glucocorticoid-mediated autophagy. Mol Cell 37:257-263.

Bianco P, Robey PG, Simmons PJ (2008) Mesenchymal stem cells: revisiting history, concepts, and assays. Cell Stem Cell 2:313-319.

Chin TY, Kao CH, Wang HY, Huang WP, Ma KH, Chueh SH (2010) Inhibition of the mammalian target of rapamycin promotes cyclic AMP-induced differentiation of NG108-15 cells. Autophagy 6:1139-1156.

Cho KJ, Trzaska KA, Greco SJ, McArdle J, Wang FS, Ye JH, Rameshwar P (2005) Neurons derived from human mesenchymal stem cells show synaptic transmission and can be induced to produce the neurotransmitter substance P by interleukin-1 alpha. Stem Cells 23:383-391.

Coolen M, Thieffry D, Drivenes Ø, Becker TS, Bally-Cuif L (2012) miR-9 controls the timing of neurogenesis through the direct inhibition of antagonistic factors. Dev Cell 22:1052-1064.

Dajas-Bailador F, Bonev B, Garcez P, Stanley P, Guillemot F, Papalopulu N (2012) MicroRNA-9 regulates axon extension and branching by targeting Map1b in mouse cortical neurons. Nat Neurosci 15:697-699.

Ding Y, Choi ME (2014) Regulation of autophagy by TGF-β: emerging role in kidney fibrosis. Semin Nephrol 34:62-71.

Elramah S, Landry M, Favereaux A (2014) MicroRNAs regulate neuronal plasticity and are involved in pain mechanisms. Front Cell Neurosci 8:31.

Han R, Kan Q, Sun Y, Wang S, Zhang G, Peng T, Jia Y (2012) MiR-9 promotes the neuronal differentiation of mouse bone marrow mesenchymal stem cells via targeting zinc finger protein 521. Neurosci Lett 515:147-152.

Jia GQ, Zhang MM, Yang P, Cheng JQ, Lu YR, Wu XT (2009) Effects of the different culture and isolation methods on the growth, proliferation and biology characteristics of rat bone marrow mesenchymal stem cells. Sichuan Da Xue Xue Bao Yi Xue Ban 40:719-723.

Jian X, Xiao-yan Z, Bin H, Yu-feng Z, Bo K, Zhi-nong W, Xin N (2011) MiR-204 regulate cardiomyocyte autophagy induced by hypoxia-reoxygenation through LC3-II. Int J Cardiol 148:110-112.

Jing L, Jia Y, Lu J, Han R, Li J, Wang S, Peng T, Jia Y (2011) MicroRNA-9 promotes differentiation of mouse bone mesenchymal stem cells into neurons by Notch signaling. Neuroreport 22:206-211.

Krichevsky AM, Sonntag KC, Isacson O, Kosik KS (2006) Specific microRNAs modulate embryonic stem cell-derived neurogenesis. Stem Cells 24:857-864.

Lee JA, Kim BI, Jo CH, Choi CW, Kim EK, Kim HS, Yoon KS, Choi JH (2010) Mesenchymal stem-cell transplantation for hypoxic-ischemic brain injury in neonatal rat model. Pediatr Res 67:42-46.

Levine B, Klionsky DJ (2004) Development by self-digestion: molecular mechanisms and biological functions of autophagy. Dev Cell 6:463-477.

Li F, Li L, Zhong Y, Xie Q, Huang J, Kang X, Wang D, Xu L, Huang T (2013) Relationship between LTR methylation and gag expression of HIV-1 in human spermatozoa and sperm-derived embryos. PLoS One 8:e54801.

Lu C, Chen J, Xu HG, Zhou X, He Q, Li YL, Jiang G, Shan Y, Xue B, Zhao RX, Wang Y, Werle KD, Cui R, Liang J, Xu ZX (2014) MIR106B and MIR93 prevent removal of bacteria from epithelial cells by disrupting ATG16L1-mediated autophagy. Gastroenterology 146:188-199.

Michaeli S, Galili G (2014) Degradation of organelles or specific organelle components via selective autophagy in plant cells. Int J Mol Sci 15:7624-7638.

Mizushima N, Levine B, Cuervo AM, Klionsky DJ (2008) Autophagy fights disease through cellular self-digestion. Nature 451:1069-1075.

Mizushima N, Yoshimori T (2007) How to interpret LC3 immunoblotting. Autophagy 3:542-545.

Petherick KJ, Williams AC, Lane JD, Ordóñez-Morán P, Huelsken J, Collard TJ, Smartt HJ (2013) Autolysosomal β-catenin degradation regulates Wnt-autophagy-p62 crosstalk. EMBO J 32:1903-1916.

Ryter SW, Mizumura K, Choi AM (2014) The impact of autophagy on cell death modalities. Int J Cell Biol 2014:502676.

Tan SL, Ohtsuka T, González A, Kageyama R (2012) MicroRNA9 regulates neuronal stem cell differentiation by controlling Hes1 expression dynamics in the developing brain. Genes Cells 17:952-961.

Vázquez P, Arroba AI, Cecconi F, de la Rosa EJ, Boya P, de Pablo F (2012) Atg5 and ambra1 differentially modulate neurogenesis in neuronal stem cells. Autophagy 8:187-199.

Vessoni AT, Muotri AR, Okamoto OK (2012) Autophagy in stem cell maintenance and differentiation. Stem Cells Dev 21:513-520.

Wan G, Xie W, Liu Z, Xu W, Liao M, He J, Jiang Y, Yang BB, Xu H, Xu N, Zhang Y (2014) Hypoxia-induced MIR155 is a potent autophagy inducer by targeting multiple players in the MTOR pathway. Autophagy 10:70-79.

Wang J, Yang K, Zhou L, Minhaowu, Wu Y, Zhu M, Lai X, Chen T, Feng L, Li M, Huang C, Zhong Q, Huang X (2013) MicroRNA-155 promotes autophagy to eliminate intracellular mycobacteria by targeting Rheb. PLoS Pathog 9:e1003697.

Woodbury D, Schwarz EJ, Prockop DJ, Black IB (2000) Adult rat and human bone marrow stromal cells differentiate into neurons. J Neurosci Res 61:364-370.

Xu X, Fu Y, Tong J, Fan S, Xu K, Sun H, Liang Y, Yan C, Yuan Z, Ge Y (2014) MicroRNA-216b/Beclin 1 axis regulates autophagy and apoptosis in human Tenon's capsule fibroblasts upon hydroxycamptothecin exposure. Exp Eye Res 123:43-55.

Yang L, Chao J, Kook YH, Gao Y, Yao H, Buch SJ (2013) Involvement of miR-9/MCPIP1 axis in PDGF-BB-mediated neurogenesis in neuronal progenitor cells. Cell Death Dis 4:e960.

Yu L, Alva A, Su H, Dutt P, Freundt E, Welsh S, Baehrecke EH, Lenardo MJ (2004) Regulation of an ATG7-beclin 1 program of autophagic cell death by caspase-8. Science 304:1500-1502.

Zeng M, Zhou JN (2008) Roles of autophagy and mTOR signaling in neuronal differentiation of mouse neuroblastoma cells. Cell Signal 20:659-665.

Zhang GY, Wang CQ, Peng Y, Peng T, Jia YJ (2013) Function of autophagy on differentiation of rat bone marrow mesenchymal stem cells into neurons. Zhongguo Ying Yong Sheng Li Xue Za Zhi 29:389-390, 394.

Zhang J, Liu J, Huang Y, Chang JY, Liu L, McKeehan WL, Martin JF, Wang F (2012) FRS2α-mediated FGF signals suppress premature differentiation of cardiac stem cells through regulating autophagy activity. Circ Res 110:e29-39.

Zhao C, Sun G, Li S, Shi Y (2009) A feedback regulatory loop involving microRNA-9 and nuclear receptor TLX in neuronal stem cell fate determination. Nat Struct Mol Biol 16:365-371.

Zhao Y, Huang Q, Yang J, Lou M, Wang A, Dong J, Qin Z, Zhang T (2010) Autophagy impairment inhibits differentiation of glioma stem/progenitor cells. Brain Res 1313:250-258.

Zhao Y, Chen G, Zhang W, Xu N, Zhu JY, Jia J, Sun ZJ, Wang YN, Zhao YF (2012) Autophagy regulates hypoxia-induced osteoclastogenesis through the HIF-1α/BNIP3 signaling pathway. J Cell Physiol 227:639-648.

Zhu H, Wu H, Liu X, Li B, Chen Y, Ren X, Liu CG, Yang JM (2009) Regulation of autophagy by a beclin 1-targeted microRNA, miR-30a, in cancer cells. Autophagy 5:816-823.

Copyedited by Aprico K, Maxwell R, Wang J, Qiu Y, Li CH, Song LP, Zhao M